NASA Technical Memorandum 103166
AIAA-90-2241

A Comparison of Analytical Results for 20 K LOX/Hydrogen Instabilities

Mark D. Klem and Kevin J. Breisacher
Lewis Research Center
Cleveland, Ohio

Prepared for the
26th Joint Propulsion Conference
cosponsored by the AIAA, SAE, ASME, and ASEE
Orlando, Florida, July 16-18, 1990

NASA

A COMPARISON OF ANALYTICAL RESULTS FOR 20K LOX/HYDROGEN INSTABILITIES

Mark D. Klem[1] and Kevin J. Breisacher[1]
NASA Lewis Research Center
Cleveland, Ohio

Abstract

Test data from NASA Lewis' "Effect of Thrust Per Element on Combustion Stability Characteristics of Hydrogen-Oxygen Rocket Engines" test program are used to validate two recently released stability analysis tools. The first tool is a design methodology called ROCCID (ROCket Combustor Interactive Design). ROCCID is an interactive design and analysis methodology that uses existing performance and combustion stability analysis codes. The second tool is HICCIP (High frequency Injection Coupled Combustion Instability Program). HICCIP is a recently developed combustion stability analysis model. Using a matrix of models, results from analytic comparisons with 20K LOX/H_2 experimental data are presented.

Introduction

In order to provide a convenient tool for the analysis and design of liquid rocket engine combustors, NASA Lewis initiated "LOX/Hydrocarbon Rocket Engine Analytical Design Methodology and Validation," NAS 3-25556. The purpose of this program was to compile and evaluate existing codes, select the most appropriate codes for an interactive program, and provide a modular framework that would make these codes readily usable. The product of this effort is ROCCID (ROCket Combustor Interactive Design). ROCCID is currently capable of analyzing mixed element injector patterns containing impinging like-doublet, impinging triplet, showerhead, shear coaxial, and hydraulic hollow-cone swirl coaxial elements. Real propellant properties for liquid and gaseous oxygen, hydrogen, methane, propane, and liquid RP-1 are currently available. ROCCID also contains the logic to interactively create a combustor design which will meet input performance and stability goals.

Currently, ROCCID has been released to industry for their use and their assistance in identifying any problems that may still exist in the code (i.e., BETA test). As part of this "BETA test" process, the authors selected a set of instability data and ran ROCCID through its matrix of available models both as an operational test of ROCCID and as a quick comparison of the range of results obtained by running existing models for the same problem. It should be made clear that it is not the intent of the authors to indicate one model as being superior to another. Rather, our intent is to illustrate the qualitative nature of the state of the art of combustion instability analyses and to demonstrate the convenience of using a framework such as ROCCID for making model comparisons.

HICCIP (High frequency Injection Coupled Combustion Instability Program) (Ref. 1), a recently developed combustion stability model, was also used to analyze the same set of data. HICCIP is in its validation phase and further refinements to the code are planned in the future. The analysis of these tests and comparisons to existing models provide a means of validating HICCIP at this stage in its development.

Description of the Models

The matrix of models utilized in ROCCID to analyze the stability of the 20K

[1]Member AIAA

combustors is shown in Table I.

HIFI (High Frequency Intrinsic Stability Analysis) (Ref. 2) utilizes a concentrated (at a single axial plane) combustion model and the sensitive time-lag approach. In the concentrated combustion approach, the combustion chamber is divided into two regions: the region upstream of the combustion plane where the mean velocity is assumed to be zero and a region downstream of the combustion plane where the velocity is assumed to be non-zero and constant. Using the separation of variables technique, a general solution governing the velocity potential function (obtained by combining the continuity and momentum equations and an isentropic pressure/density relationship) can be obtained. The injector face boundary condition is applied to calculate the chamber admittance (the perturbation in velocity divided by the perturbation in pressure) upstream of the combustion plane. Using the nozzle admittance as a boundary condition, the chamber admittance downstream of the combustion plane is calculated. Continuity is then applied at the combustion plane to relate the burning admittance to the upstream and downstream chamber admittances. The pressure interaction index, n, and the sensitive time lag, t, for neutral stability can then be calculated using an expression derived by Crocco (Ref. 3).

The 3D Distributed Combustion Model (DIST3D) (Ref. 2) contains a more detailed model of the chamber acoustics that can include the effects of stability aids (absorbers and baffles) and a more realistic treatment of the combustion zone. The combustion zone is modeled as being distributed over a significant portion of the combustor. The combustion zone parameters (chamber acoustic velocity, chamber gas velocity, etc.) are modeled in a piecewise-linear fashion. The features for stability aids are not used in the current analyses.

The Combustion Response Prediction (CRP) model (Ref. 2) calculates the open-loop response of the burning rate to a specified acoustic oscillation in the combustion chamber. Using analytical solutions for the pressure and velocity fluctuations in a closed cylinder, the pressure and velocity histories for a specific instability mode can be calculated. With the pressure and velocity fields specified, the vaporization history for a droplet can be calculated using Ranz-Marshall (Ref. 4) correlations for the heat and mass transfer coefficients and assuming the transfer processes are quasi-steady state. Using an energy balance, the temporal variations of the drop diameter, temperature (assumed uniform), and the vaporization rate can be calculated. The continuous injection of propellant is simulated as arrays of single drops that are injected from various radial, circumferential and temporal locations. An in-phase and out-of-phase combustion response can then be calculated.

The Lumped Parameter Injection Response Model (INJ) (Ref. 2) is similar to that described in Reference 5. The injection element admittance is characterized by its resistance, capacitance and inertance terms. It is assumed in INJ that the wavelength of an element oscillation is much larger than the elements physical dimensions.

In the Lewis Injection Response Model (LEINJ) (Ref. 2), flow and pressure oscillations in the tubes of a coaxial injector element are determined by solving the one dimensional mass and momentum conservation equations as a function of axial position. Pressure losses in the orifice are modeled using a discharge coefficient. Oscillations in the manifolds are described by the three dimensional wave equation for finite Mach number flow solved by using the separation of variables technique.

SMITH-REARDON refers to the widely used N-tau correlation developed in the 1960's (Ref. 6). AEROJET 20% Vaporized is an analytical procedure developed to calculate the sensitive time-lag (Ref. 2).

AEROJET and DROPMIX are two of the drop size correlations currently available in ROCCID for coaxial injectors.

HICCIP Description

HICCIP treats flow oscillations, produced by chamber pressure oscillations, in both the fuel and oxidizer elements using the same approach as outlined for LEINJ.

The atomization process was followed on a quasi-steady basis using the relations of Mayer for coaxial injection as described in Reference 1. Instantaneous local velocities were determined at various times in an oscillation cycle. The atomization rate and drop size produced in the combustion chamber were calculated for conditions corresponding to these velocities. An effective atomization plane was established at the location where 50% of the mass of the jet has been atomized. The vaporization process was assumed to begin at this effective atomization plane.

The mean drop size of the spray was specified as the mass average of the drops produced at various locations in the combustor. Drop size groups are calculated using the mean drop size and a log normal distribution. Normally, 11 drop size groups are used to calculate steady state performance and 5 drop size groups are used for instability calculations. The quasi-steady vaporization theory of Reference 7 was modified to include finite thermal conductivity by calculating the heat transfer between shells within each drop. The influence of internal droplet circulation was approximated by multiplying the physical thermal conductivity by a factor of 2.7. Injection of drops was considered to occur at 30 discrete intervals during a cycle of oscillation. The average and oscillating burning rate during a cycle are determined at 30 axial locations. The drops were injected at a radial location corresponding to the median area and at a single angular location.

Gas phase oscillations in the chamber were calculated assuming distributed combustion and by using a wave equation solved by separation of variables. Between axial locations in the combustor, the oscillation profiles were calculated using this wave equation. At the various axial stations, the average and oscillating velocity components were adjusted to account for the average and oscillating burning rates. An iterative solution technique is necessary to obtain the same burning rates from the vaporization calculations as those used in the wave dynamic calculations. The wave dynamic calculations begin at the nozzle and proceed to the injector with an assumed average burning rate response. If the velocity at the injector face was not zero, a new average burning rate response was assumed. The calculations were then repeated with different frequencies (real and imaginary) until the average burning rate response (the in and out-of-phase components) agreed with the vaporization rate calculations. The local speed of sound used in the wave dynamics calculations varied as a function of axial position based on the amount of burning that had occurred by that position. Oscillations at the nozzle end of the chamber, were assumed to follow those for an ideal, short-distributed nozzle.

Experimental Data

The experimental data chosen to be used for model comparisons were the data generated in Reference 8. This data set was chosen for several reasons. First, there is significant documentation of the hardware specifications and operating conditions for meaningful comparisons to be made. Second, these data are not included in the sets of test cases used in the development of ROCCID. Finally, the absence of stability aids (absorbers or baffles) in the combustor permits comparisons to be made with HICCIP.

The hardware used in Reference 8 are 20K-lbf-thrust Liquid Oxygen (LOX)/H_2 engines operated at a nominal chamber pressure of

300 psi. Six coaxial injector configurations were tested. The thrust per element varied from 20 to 1000 lbf. The chamber consisted of a 10.78 inch diameter heat sink cylindrical section bolted to a convergent-divergent heat-sink nozzle. Stability characteristics were mainly determined using hydrogen temperature ramping (several of the injectors that were still stable at the lowest obtainable H_2 injection temperature were bombed (pulsed using an explosive charge). The stability of the combustors was characterized by a H_2 injection transition temperature. The transition temperature was defined as the H_2 injection temperature where unstable combustion was first encountered.

The results of this test program are summarized in Table II. Three of the six injectors (992, 397, and 201 elements) were driven unstable during temperature ramping. The 100, 35, and 20 element injectors did not have a discernible transition temperature in the range of hydrogen temperatures tested. No further analysis was attempted for these injectors because they do not provide a very useful test for the codes. The 992, 397, and 201 element injectors all encountered instabilities during temperature ramping. Reference 8 provides strip chart traces of a typical instability for each of these three injectors (Fig. 1). These traces indicate the acoustic mode, frequency, and peak-to-peak limit amplitude of the instabilities encountered. The 992 element injector is of particular interest in that the temperature ramping did not induce the "usual" first tangential (1T) mode but excited the second tangential (2T) mode (Fig. 1). This is of interest because in a recent test program with methane, temperature ramping failed to induce the 1T mode but consistently excited a higher order mode. The 992 element injector was chosen as the focal point for these analyses.

ROCCID Results

The absence of stability aids and the use of input parameters generated by the existing logic in ROCCID (i.e. no "tweaking") provide a very stringent test of the models in ROCCID. The ability of ROCCID to provide stability margin by the design of stability aids (its strongest feature) is not demonstrated. There was one major drawback with choosing to analyze the 20K LOX/H_2 data with ROCCID. The INJ model in ROCCID is hardwired to analyze coaxial elements in which the orifice is located at the top of the LOX tube upstream of a substantial diffuser section (Fig. 2). This configuration represents the so called "modern" injection element. Unfortunately, the elements in the 20K LOX/H_2 engine had orifices at the exit of the elements with no diffuser section. To remedy this situation, a very short (10^{-6} inch), fictitious diffuser section was added downstream of the orifice. The width of this diffuser section was then adjusted until reasonable agreement was obtained with experimental pressure drop data. Adjusting this fictitious diffuser section width did not significantly affect the predicted drop size. The location of the orifice in an element is not a problem when using the LEINJ module.

Tables III and IV show the performance and stability characteristics for the matrix of ROCCID models run in the study. The arrangement of the table is based upon the increased detail or mechanistic approach of the models utilized. It should be noted that with the interactive framework of ROCCID, once the geometry and operating conditions for an engine are input, different analysis modules can be selected by interactively setting the appropriate switches. With the exception of CRP, the computer runtimes associated with these modules are sufficiently short that a substantial matrix of models can be run in an afternoon.

The experimental performance data for the 20K LOX/H_2 engine is somewhat erratic. An examination of Table II shows that C* efficiencies in excess of 100% were reported. Unfortunately, the C* reported for test 0002 is probably erroneous due

to incorrect hydrogen weight flows resulting from mixing tube storage. Additional performance data reported in Reference 8 indicates that the 992 element injector is characterized by a C* efficiency of approximately 99.7% during stable operation. During temperature ramping, the C* efficiency of the 992 element injector is approximately 96%. The C* efficiencies calculated by the performance modules of ROCCID are in reasonable agreement with those observed experimentally. This is despite the fact that the drop sizes calculated by two of the available correlations can disagree by more than a factor of three. This is not an uncommon occurrence for the drop size correlations in ROCCID. Both correlations generally predict a larger drop size and lower performance for the temperature ramped test case 0002. However, when DROPMIX is used in conjunction with LEINJ this trend is reversed. This is similar to the trend observed with HICCIP.

There was a wide range of calculated stability results obtained as indicated in Table IV. For all the models where an instability is indicated (growth rate (λ) greater than 0), the ratio of burning admittance (YB) to injector admittance (YJ) is less than one (indicating an injection coupled instability). The cases run with LEINJ indicate an even more pronounced injector influence (even smaller values of YB/YJ).

For test case 0001, fourteen of the eighteen different model combinations correctly predict stable tests. For test case 0002, only six of the eighteen combinations predict a 2T instability. Of those six, the predicted frequency varies by $\pm$1000 Hz. from the frequency that was reported in Reference 8.

The influence of calculated drop size on stability results is demonstrated by examining the first two model entries in Tables III and IV. Using the same chamber acoustics, injection, and combustion models but changing the drop size correlation model, the mode of the calculated instability switched. It is also interesting that erroneous 1R and 3T modes occurred only when using the smaller calculated drop size (AEROJET). The use of LEINJ might be expected to make the 2T instability more prominent (due to the resonance at 4100 Hz indicated in Fig. 3), but this was not observed. In fact, LEINJ seemed to increase the occurrence of a calculated 1T instability (Table IV HNLAS, HNLDS, and HCLA). In general, it might be expected that as one proceeds down Table IV (increasing model complexity) better agreement would be obtained between experimental and analytical results, but this is not the case.

HICCIP Results

A review of the reports from the NASA LeRC LOX/H_2 stability programs of the 1960's shows that modes other than the 1T have occurred but not as frequently as 1T. Indeed, if as indicated below that LOX tube coupling plays a significant role in the occurrence of these other modes, then the repeated use of hardware with similar injection element dimensions may account for the occurrence of these modes.

The performance module in HICCIP calculated C* efficiencies of 97% and 99% using drop sizes (D_{30}) of 172 microns and 90 microns for test cases 0001 and 0002 respectively. Currently, there are no correlations for the constants in the relations for drop size or atomization rate in HICCIP. These constants are the two remaining "knobs" that are tweaked that limit the pre-test applicability of the code.

Figure 1a shows the amplitude spectral density traces for test 0002 with the 992 element injector. At a hydrogen transition temperature of 78°R, a second tangential instability was excited and grew to a 150 psi peak-to-peak amplitude at a frequency of approximately 5420 Hz. There was also some activity at approximately 3200 Hz with an amplitude of 28 psi peak-to-peak. Figure 3 shows the normalized response (normalized by

the ratio of chamber pressure to flowrate) of the LOX injection element for the first and second tangential modes for test case 0002. The LOX tube has a resonance at approximately 4100 Hz. The LOX side response is near a minimum at the 1T frequency for the chamber (3435 Hz assuming thoroughly mixed gas composition). Although the resonance for the LOX system is well below the 2T frequency for the chamber (5697 Hz), during ramping, the injection of the cold hydrogen can substantially reduce the local acoustic velocity at the injector face (Ref. 9). This can allow the LOX post to tune with the chamber and initiate an instability that shifts in frequency as it grows in amplitude. This is apparently what happened in the case of the 40K LOX/methane 1T instabilities. The sharp spike in Figure 3, occurring at approximately 2700 Hz, is due to a resonance in the LOX manifold. These resonances generally have such a small bandwidth that they have difficulty initiating and sustaining an instability.

The fuel side response for the stable test 0001 and the unstable reduced hydrogen injection temperature test 0002 are shown in Figure 4. Figure 4 clearly shows the significant increase in fuel side response as the hydrogen injection temperature is reduced (test 0002). The fuel side response also shows a significant change as a function of frequency for the reduced temperature case. The maximum response occurs near the 2T chamber frequency (5697 Hz).

While the response plots for the injection elements may provide some insight into why, and if a particular instability mode occurs, they are not an absolute indicator. The graphs only show the magnitude of the injection response and not the phase relationship with other processes. HICCIP attempts to account for the phasing and magnitude relationships of the dominant physical processes occurring during an instability.

Figures 5 - 8 show the HICCIP results for the 992 element injector. The regions exhibiting a negative damping rate are unstable. Figures 5 and 6 indicate the ambient hydrogen temperature case (test 0001) would be stable until an approximately 35 psi half-amplitude (half the peak-to-peak value) organized disturbance would be introduced into the combustor. From the HICCIP results, it would be expected that this case would be spontaneously stable, which conforms with experimental observations. Unfortunately, the 992 element injector was never bombed. A higher amplitude disturbance might have induced an instability. Figures 7 and 8 are the HICCIP results for the 1T and 2T modes respectively for test case 0002 which was ramped unstable. The 1T results indicate an instability at this hydrogen injection temperature that grows to a limit cycle amplitude (ie. where the damping rate curve crosses from negative to positive) of approximately 30 psi (60 psi peak-to-peak) at approximately 3100 Hz (the point on the frequency curve corresponding to the zero of the damping rate curve). This overestimates the magnitude of the 1T activity observed by a factor of 2 (Fig. 1). However, the frequency calculated for the 1T is in good agreement with the data. Since the growth rates for the 2T oscillation are substantially larger than those for the 1T oscillation, it is possible the test was terminated before the 1T oscillation reached its limit cycle amplitude. The results for the 2T mode exhibit an instability that grows to 80 psi (160 psi peak-to-peak) at approximately 5580 Hz. Although the frequency predicted for the 2T mode is above the 5420 Hz observed (the HICCIP results are closer to the equilibrium value of 5697 Hz), the limit cycle amplitude results are in good agreement with experiment (Fig. 1). Figure 8 also indicates that the frequency at which a small amplitude (5 - 10% of chamber pressure) disturbance begins to grow is between 4000 - 4200 Hz (the region of resonance for the LOX tube).

Conclusions

The interactive nature of ROCCID provides a powerful framework for making comparisons with existing combustion instability models.

The qualitative nature of the unanchored use of the instability modules in ROCCID is apparent. The models' pre-test predictive capabilities are questionable.

Additional drop size correlations and/or guidelines for the range of parameters the correlations are valid over should be incorporated in ROCCID.

HICCIP analyses indicate that LOX tube acoustic resonance probably played a significant role in the occurrence of the 2T mode of the 992 element injector.

HICCIP can provide some insight into the mechanisms that may cause an instability to occur. However, further refinement of HICCIP is required to make it a useful pre-test analysis tool.

References

1. Priem, R.J., and Breisacher, K.J., "Nonlinear Combustion Instability Model in Two- to Three-Dimensions," NASA TM-102381, 1989.

2. Muss, J.A., and Johnson, C.W., "LOX/Hydrocarbon Rocket Analytical Design Methodology Development Validation, NAS 3-25556, ROCCID User's Manual, NASA CR-185187, 1990.

3. Crocco, L., and Cheng, S., Theory of Combustion Instability in Liquid Propellant Rocket Motors, Butterworths Scientific Publications, London, 1956.

4. Ranz, W.E., and Marshall, W.R., Jr., "Evaporation from Drops," Chemical Engineering Progress, Vol. 48, No. 3, Mar. 1952, pp. 141-146.

5. Harrje, D.T., and Reardon, F.H., eds., "Liquid Propellant Rocket Combustion Instability," NASA SP-194, 1972.

6. Smith, A.L., and Reardon, F.H., "The Sensitive Combustion Time Lag Theory and Its Application to Liquid Rocket Combustion Instability Problems," (Vol. 1 Engineer's Manual) TR-AFRPL-TR-67-314, 1968.

7. Priem, R.J., and Heidmann, M.F., "Propellant Vaporization as a Design Criterion for Rocket Engine Combustion Chambers," NASA TR-R-67, 1960.

8. Salmi, R.J., Wanhainen, J.P., and Hannum, N.P., "Effect of Thrust Per Element on Combustion Stability Characteristics of Hydrogen-Oxygen Rocket Engines," NASA TN D-4851, 1968.

9. Jensen, R.J., Dodson, H.C., and Claflin, S.E., "LOX/Hydrocarbon Instability Investigation," NASA CR-182249, 1989.

Table I
ROCCID Models

Chamber Acoustics	Combustion Response	Injector Admittance	Drop Size Correlation	TAU Correlation
HIFI DIST3D	CRP N-TAU	INJ LEINJ	AEROJET DROPMIX	AEROJET 20% SMITH-REARDON

TABLE II. - STABILITY DATA

TEST	Number of elements, E	Hydrogen-injection temperature, T		Oxidant to fuel ratio, O/F	Chamber pressure at injector, P_c		Total propellant weight flow, $\dot{\omega}_p$		Hydrogen-injector pressure drop, ΔP_h		Oxygen injector pressure drop, ΔP_0		Hydrogen injector velocity, V_h		Injection velocity ratio, V_h/V_0	Characteristic velocity efficiency, $\eta_{c'}$ percent	Remarks
		°R	K		psia	N/m^2	lb/sec	kg/sec	psi	N/m^2	psi	N/m^2	ft/sec	m/sec			
0001	992	124	68.9	5.138	310	2137×10^3	59.97	27.20	45	311×10^3	354	2441×10^3	735	224	4.93	100.6	Stable
0002		78	43.3	5.25	292	2013	61.08	27.71	15	103	381	2627	378	115	2.44	[a]92.7	Transition
0003		101	56.1	4.069	312	2151	59.42	26.95	42	289	358	2468	645	197	4.46	98.9	
0004		80	44.1	5.72	294	2027	63.00	28.58	14	97	389	2682	383	117	2.36	[a]92.3	
0005		82	45.6	3.769	308	2123	60.05	27.24	31	214	318	2193	483	147	3.95	95.9	
0006		98	54.4	4.478	309	2130	60.70	27.53	38	262	335	2309	599	183	3.99	96.8	
0007		109	60.6	6.52	298	2055	63.17	28.65	27	186	397	2737	563	172	3.40	96.1	
0008		89	49.4	4.77	306	2109	61.82	28.04	30	207	348	2399	497	152	3.21	94.6	
0009	397	114	63.3	4.86	317	2186×10^3	58.96	26.74	49	338×10^3	136	937×10^3	911	278	12.56	102.3	Stable
0010		66	36.7	4.84	348	2399	67.22	30.45	15	103	180	1241	825	252	1.15	98.0	Transition
0011		68	37.8	3.833	326	2248	64.87	29.43	18	124	157	1082	724	221	1.50	93.1	
0012		65	36.1	5.67	337	2323	68.35	31.00	11	76	191	1317	678	207	.79	96.3	
0013		64	35.6	6.15	336	2317	71.46	32.41	10	69	217	1496	711	217	.89	(b)	
0014	201	60	33.3	3.72	319	2199×10^3	58.60	26.58	15	103×10^3	324	2234×10^3	151	46	1.00	97.2	Stable
0015		62	34.4	4.27	316	2178	61.17	27.75	10	69	336	2317	147	45	.95	96.4	Stable
0016		62	34.4	4.69	316	2178	59.67	27.07	9	62	329	2268	132	40	.85	99.8	Transition
0017		64	35.6	5.06	313	2158	62.12	28.18	9	62	370	2551	151	46	.92	96.3	Stable
0018		63	35.0	4.99	312	2151	62.40	28.30	9	62	371	2558	140	43	.86	94.9	
0019		65	36.1	5.46	312	2151	65.67	29.79	7	48	425	2930	159	48	.91	91.9	
0020		60	33.3	3.65	315	2171	60.48	27.43	11	76	299	2062	154	47	1.03	96.2	
0021	100	59	32.8	4.23	288	1985×10^3	56.03	25.42	8	55×10^3	265	1827×10^3	130	40	0.74	96.6	Stable
0022		57	31.7	5.88	311	2144	67.48	30.61	8	55	423	2916	115	35	.58	92.6	Stable
0023	35	77	42.8	5.24	198	1365×10^3	54.72	24.82	30	207×10^3	541	3730×10^3	533	163	3.55	70.3	Stable
0024		65	36.1	5.03	245	1689	62.21	28.22	17	117	505	3482	273	83	1.62	75.7	
0025		68	37.8	5.07	301	2075	62.45	28.33	12	83	405	2792	223	68	1.32	92.5	
0026		58	32.2	5.27	294	2027	62.62	28.40	6	41	416	2868	121	37	.71	90.4	
0027	20	55	30.6	4.89	222	1531×10^3	66.27	30.06	12	83×10^3	367	2530×10^3	123	38	0.69	63.9	Stable
0028		56	31.1	6.07	215	1482	66.58	30.20	11	76	397	2737	105	32	.58	64.4	Stable

[a]Injector hydrogen weight flow less than indicated value because of mixing-tube storage. See PROCEDURE section.

[b]Performance data not computed due to nozzle throat erosion.

Table III
ROCCID Performance Calculations

MODELS	TEST	D30 (μ)	DELTA P_H (PSI)	DELTA P_O (PSI)	C* EFF (%)
HNIAS	0001	26.1	44.1	391.3	99.9
	0002	61.2	19.9	365.8	97.8
HNIDS	0001	85.6	45.3	401.8	98.1
	0002	117.0	21.0	385.1	94.7
HNIAA	0001	26.1	44.1	391.3	99.9
	0002	61.2	19.9	365.8	97.8
HNIDA	0001	85.6	45.3	401.8	98.1
	0002	117.0	21.0	385.1	94.7
DNIAS	0001	26.1	44.1	391.3	99.9
	0002	61.2	19.9	365.8	97.8
DNIDS	0001	85.6	45.3	401.8	98.1
	0002	117.2	20.9	385.7	94.7
DNIAA	0001	26.1	44.1	391.3	99.9
	0002	61.2	19.9	365.9	97.8
DNIDA	0001	85.6	45.3	401.8	98.1
	0002	117.0	21.0	385.1	94.7
HCIA	0001	26.1	44.1	391.3	99.9
	0002	61.2	19.9	365.8	97.8
HCID	0001	85.6	45.3	401.8	98.1
	0002	117.0	21.0	385.1	94.7
DCIA	0001	26.1	44.1	391.3	99.9
	0002	61.2	19.9	365.8	97.8
DCID	0001	85.5	45.5	402.0	98.0
	0002	117.0	21.0	385.1	94.7
HNLAS	0001	26.1	44.1	391.3	99.9
	0002	64.0	19.8	282.6	99.9
HNLDS	0001	85.6	45.3	401.8	98.1
	0002	58.9	19.2	273.9	99.8
HCLA	0001	26.1	44.1	391.3	99.9
	0002	64.0	19.8	282.7	98.1
HCLD	0001	85.6	45.3	401.8	98.1
	0002	51.7	18.1	223.8	99.8
DCLA	0001	26.1	44.1	391.3	99.9
	0002	64.0	19.8	282.6	98.1
DCLD	0001	85.6	45.3	401.8	99.4
	0002	59.0	19.2	274.2	99.8

Model designations coded as follows.
First Letter: H=HIFI, D=DIST3D;
Second Letter: C=CRP,N=N-TAU;
Third Letter: I=INJ, L=LEINJ;
Fourth Letter: A=AEROJET, D=DROPMIX;
Fifth Letter: A=AEROJET 20 %, S=SMITH-REARDON.

Table IV
ROCCID Stability Calculations

MODELS	TEST	1L λ (1/S)	1L FREQ (HZ)	1L YB/YJ	1T λ (1/S)	1T FREQ (HZ)	1T YB/YJ	2T λ (1/S)	2T FREQ (HZ)	2T YB/YJ	1R λ (1/S)	1R FREQ (HZ)	1R YB/YJ	3T λ (1/S)	3T FREQ (HZ)	3T YB/YJ
HNIAS	0001	-	-	-	-	-	-	-	-	-	-	-	-	-	-	-
	0002	NC	NC	NC	-744	4014	0.80	400	5953	0.80	-	-	-	-	-	-
HNIDS	0001	NC	NC	NC	-1387	3955	1.77	-2846	5783	0.89	-	-	-	-	-	-
	0002	-1000	3336	0.91	500	3843	0.81	-1489	7743	0.42	-	-	-	-	-	-
HNIAA	0001	-	-	-	-	-	-	-	-	-	-	-	-	-	-	-
	0002	NC	NC	NC	-767	4901	0.82	533	6026	0.91	1700	7084	0.95	1600	7542	0.94
HNIDA	0001	NC	NC	NC	-800	3426	2.41	-	-	-	-	-	-	-	-	-
	0002	-1778	1656	2.34	-	-	-	-	-	-	-	-	-	-	-	-
DNIAS	0001	-	-	-	-835	3556	NA	-	-	-	-	-	-	-	-	-
	0002	NC	NC	NC	-14	3765	NA	256	5920	NA	-	-	-	-	-	-
DNIDS	0001	NC	NC	NC	-610	3700	NA	-201	6061	NA	-	-	-	-	-	-
	0002	-1000	3334	0.90	484	3683	NA	-1250	6196	NA	-	-	-	-	-	-
DNIAA	0001	-	-	-	-	-	-	-1097	5910	NA	-	-	-	-735	8090	NA
	0002	NC	NC	NC	-25	3793	NA	506	5939	NA	1700	7084	0.95	-237	8046	NA
DNIDA	0001	NC	NC	NC	-925	3640	NA	-	-	-	-	-	-	-	-	-
	0002	-1778	1656	2.34	-	-	-	-	-	-	-	-	-	-	-	-
HCIA	0001	-	-	-	-	-	-	-	-	-	-	-	-	-	-	-
	0002	-	-	-	-	-	-	-	-	-	-	-	-	-	-	-
HCID	0001	-	-	-	-	-	-	-	-	-	-	-	-	-	-	-
	0002	-1722	3314	0.31	-22	3591	0.30	-1167	7777	0.70	-200	7690	0.67	-100	7998	0.76
DCIA	0001	-	-	-	-	-	-	-	-	-	-	-	-	-1041	8044	NA
	0002	-	-	-	-	-	-	-	-	-	-	-	-	-	-	-
DCID	0001	-	-	-	-	-	-	-	-	-	-	-	-	-	-	-
	0002	-1722	3314	0.32	-55	3702	NA	-1203	6283	NA	-200	7690	0.67	-	-	-
HNLAS	0001	-600	1034	0.23	2100	3321	0.53	NC	NC	NC	-	-	-	-	-	-
	0002	-	-	-	-1000	2642	0.37	0	4509	0.51	NC	NC	NC	-	-	-
HNLDS	0001	NC	NC	NC	2100	3145	0.44	NC	NC	NC	-	-	-	-	-	-
	0002	-	-	-	-800	2636	0.36	700	4500	0.50	NC	NC	NC	-	-	-
HCLA	0001	-	-	-	900	3247	0.01	500	5680	0.03	-	-	-	-	-	-
	0002	-	-	-	-	-	-	-	-	-	-	-	-	-	-	-
HCLD	0001	-	-	-	-	-	-	-	-	-	-	-	-	-	-	-
	0002	-	-	-	-	-	-	-	-	-	-	-	-	-	-	-
DCLA	0001	-	-	-	-	-	-	-	-	-	-	-	-	-	-	-
	0002	-	-	-	-2284	4343	NA	721	6644	NA	NC	NC	NC	2622	8588	NA
DCLD	0001	-	-	-	-	-	-	-	-	-	-	-	-	-	-	-
	0002	-	-	-	-4623	3791	NA	-	-	-	-	-	-	-	-	-

Model designations are coded as follows. First Letter: H=HIFI, D=DIST3D;
Second Letter: C=CRP, N=N-TAU; Third Letter: I=INJ, L=LEINJ;
Fourth Letter: A=AEROJET, D=DROPMIX; Fifth Letter: A=AEROJET 20%, S=SMITH-REARDON.

\- Denotes no instability found.

NC Denotes no instability converged on in allowed scanned frequency range.

NA Denotes no data available.

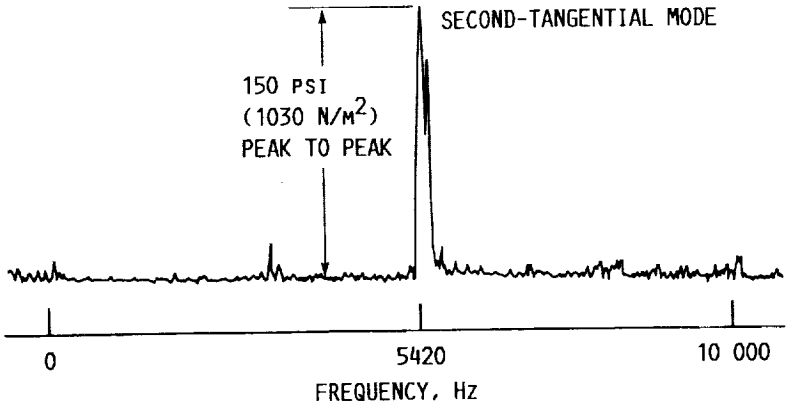

(a) 992 ELEMENTS, THRUST PER ELEMENT, 20 LB (89 N); OXIDANT-FUEL RATIO, 5.27.

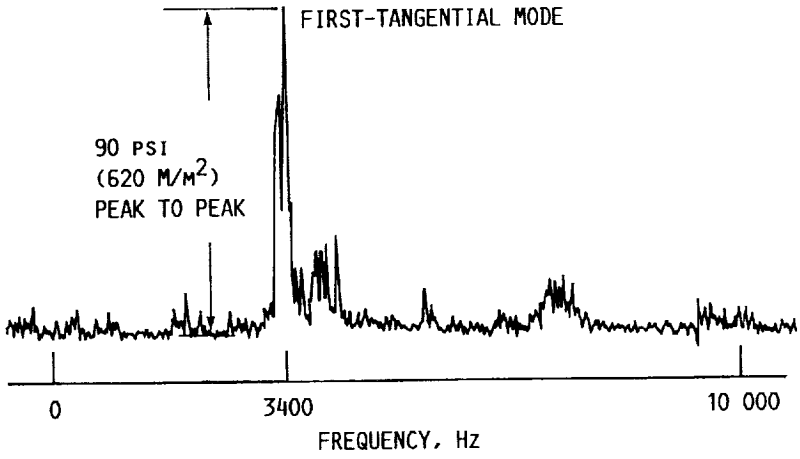

(b) 397 ELEMENTS, THRUST PER ELEMENT, 50 LB (222 N); OXIDANT-FUEL RATIO, 4.84.

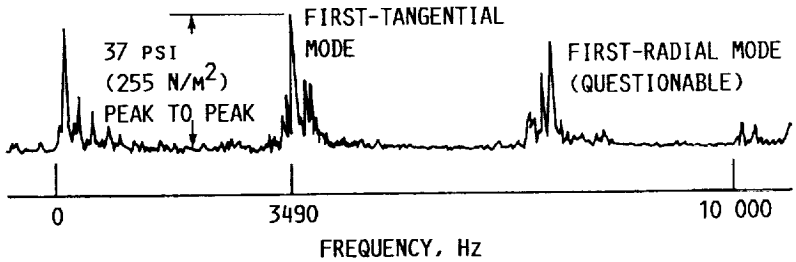

(c) 201 ELEMENTS, THRUST PER ELEMENT, 100 LB (445 N); OXIDANT-FUEL RATIO, 4.69.

FIGURE 1. - TYPICAL AMPLITUDE SPECTRAL DENSITY GRAPHS (REPRODUCED FROM NASA TN D-4851).

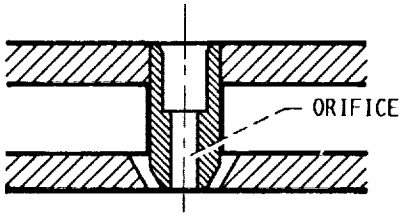

GENERAL ELEMENT

(a) NASA TN D-4851 ELEMENT DESIGN.

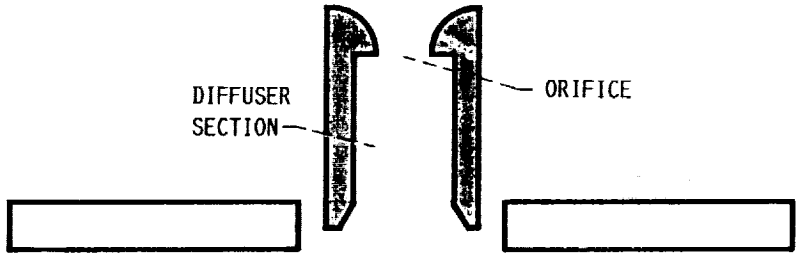

(b) ROCCID ELEMENT INPUT SCHEMATIC.

FIGURE 2. - SHEAR COAXIAL ELEMENT DESCRIPTION.

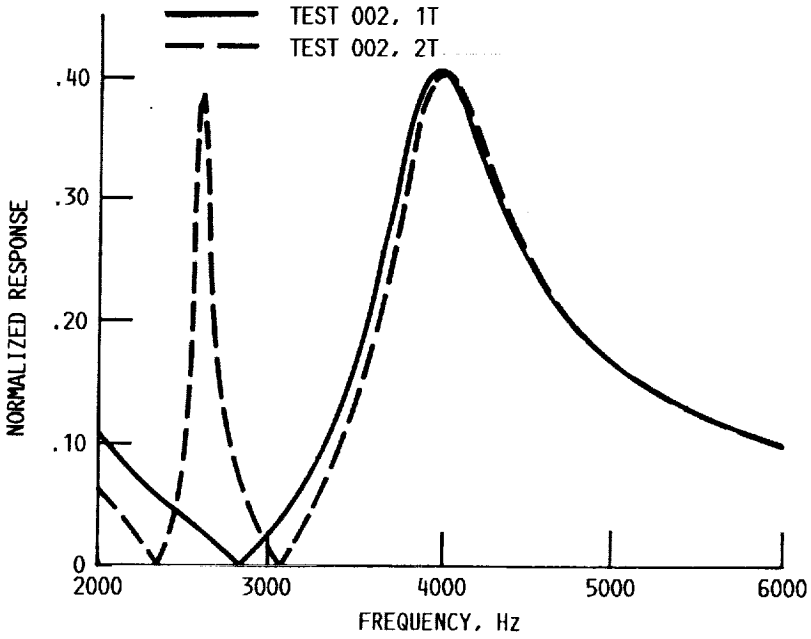

FIGURE 3. - 992 ELEMENT INJECTOR OXIDIZER SIDE RESPONSE CHARACTERISTICS.

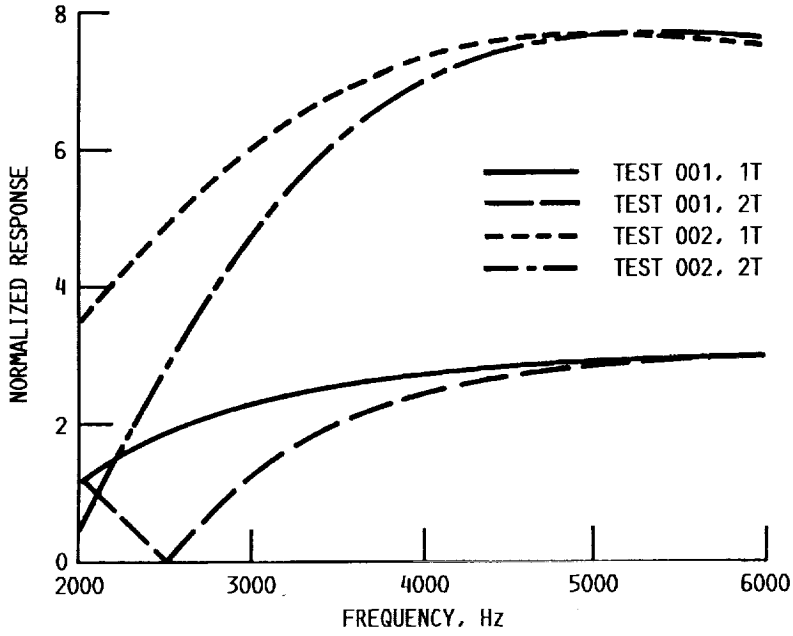

FIGURE 4. - 992 ELEMENT INJECTOR FUEL SIDE RESPONSE CHARACTERISTICS.

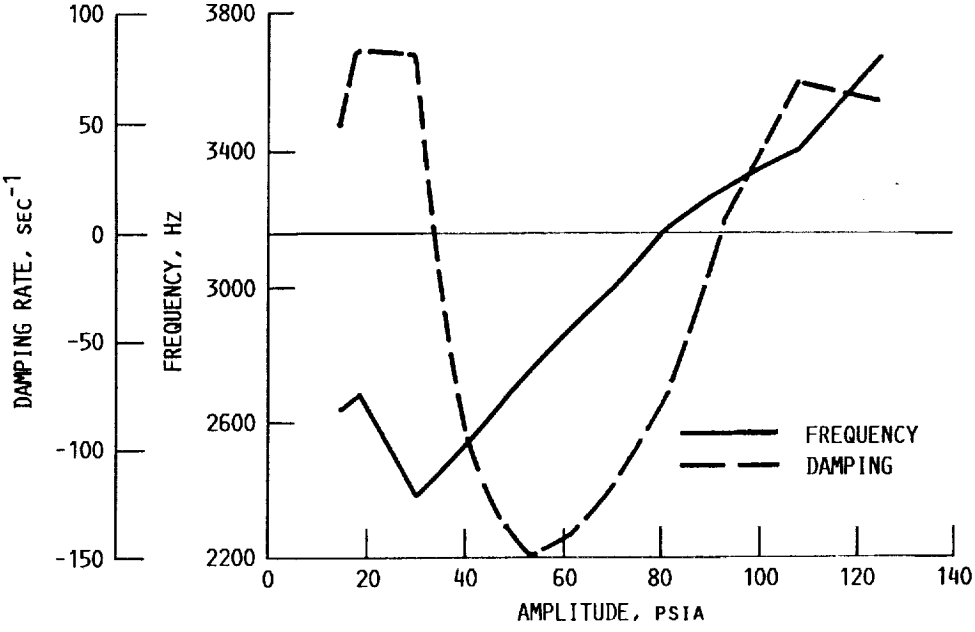

FIGURE 5. - TEST 0001 1T HICCIP STABILITY CALCULATIONS.

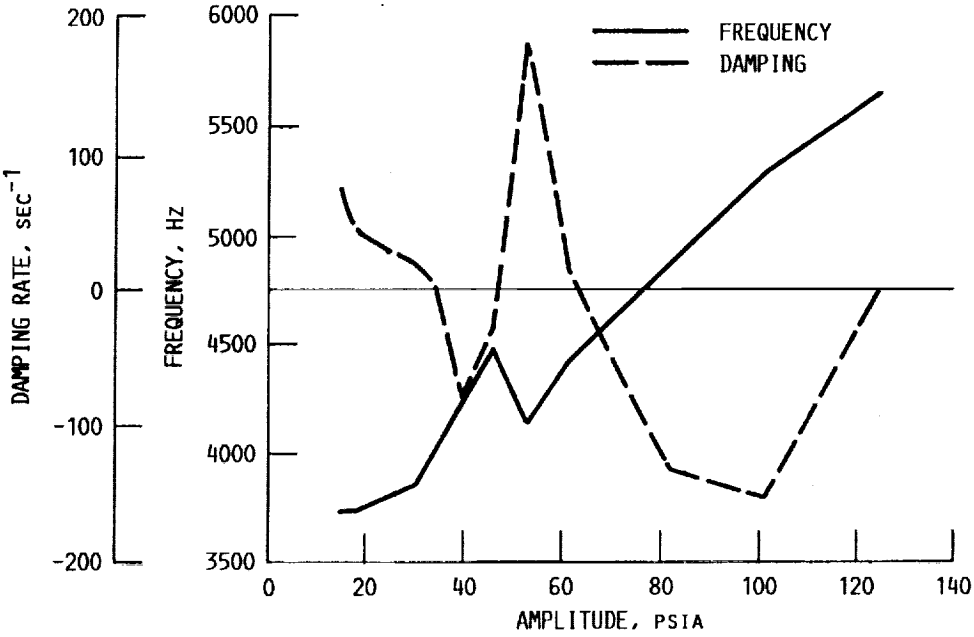

FIGURE 6. - TEST 0001 2T HICCIP STABILITY CALCULATIONS.

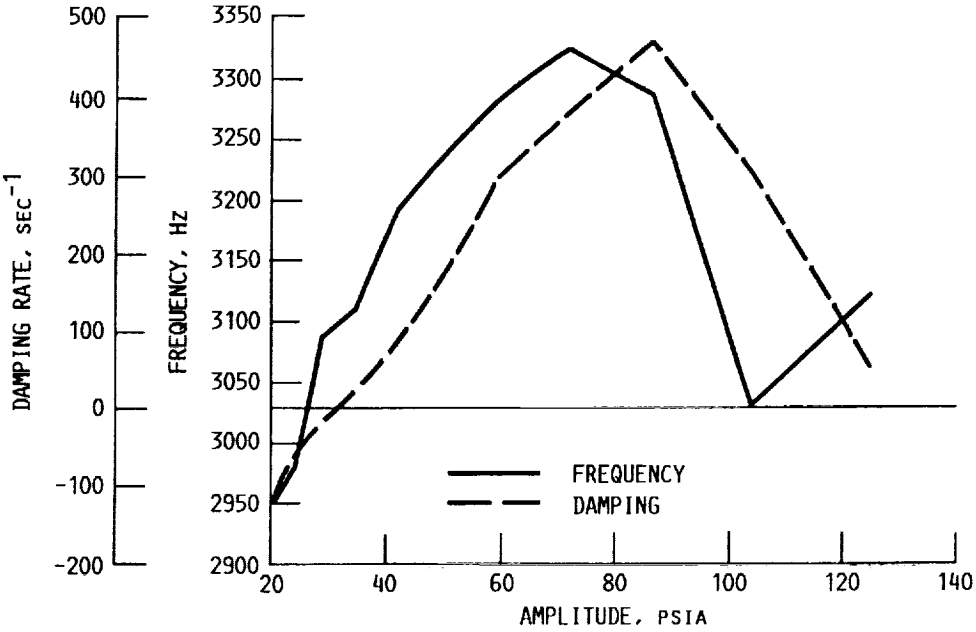

FIGURE 7. - TEST 0002 1T HICCIP STABILITY CALCULATIONS.

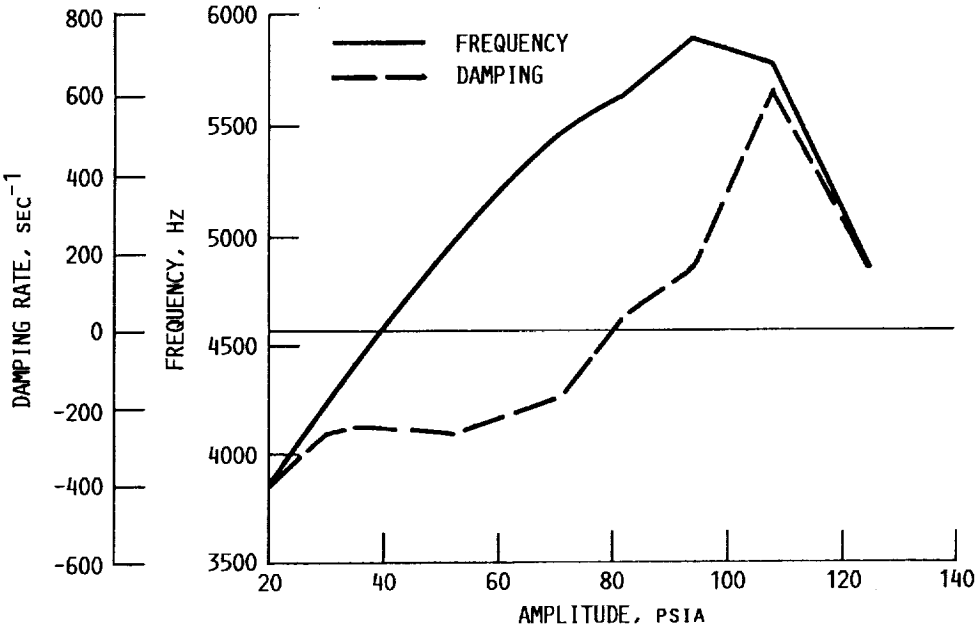

FIGURE 8. - TEST 0002 2T HICCIP STABILITY CALCULATIONS.

NASA
National Aeronautics and Space Administration

Report Documentation Page

1. Report No.	2. Government Accession No.	3. Recipient's Catalog No.
NASA TM-103166 AIAA-90-2241		

4. Title and Subtitle

A Comparison of Analytical Results for 20 K LOX/Hydrogen Instabilities

5. Report Date

6. Performing Organization Code

7. Author(s)

Mark D. Klem and Kevin J. Breisacher

8. Performing Organization Report No.

E-5538

10. Work Unit No.

582-01-21

9. Performing Organization Name and Address

National Aeronautics and Space Administration
Lewis Research Center
Cleveland, Ohio 44135-3191

11. Contract or Grant No.

13. Type of Report and Period Covered

Technical Memorandum

12. Sponsoring Agency Name and Address

National Aeronautics and Space Administration
Washington, D.C. 20546-0001

14. Sponsoring Agency Code

15. Supplementary Notes

Prepared for the 26th Joint Propulsion Conference cosponsored by the AIAA, SAE, ASME, and ASEE, Orlando, Florida, July 16-18, 1990.

16. Abstract

Test data from NASA Lewis' "Effect of Thrust Per Element on Combustion Stability Characteristics of Hydrogen-Oxygen Rocket Engines" test program are used to validate two recently released stability analysis tools. The first tool is a design methodology called ROCCID (*ROC*ket *C*ombustor *I*nteractive *D*esign). ROCCID is an interactive design and analysis methodology that uses existing performance and combustion stability analysis codes. The second tool is HICCIP (*H*igh frequency *I*njection *C*oupled *C*ombustion *I*nstability *P*rogram). HICCIP is a recently developed combustion stability analysis model. Using a matrix of models, results from analytic comparisons with 20 K LOX/H_2 experimental data are presented.

17. Key Words (Suggested by Author(s))	18. Distribution Statement
Combustion instability; Rocket; Liquid propellant engine; Combustor; Interactive design; Stability models; Computer program	Unclassified - Unlimited Subject Category 20

19. Security Classif. (of this report)	20. Security Classif. (of this page)	21. No. of pages	22. Price*
Unclassified	Unclassified	16	A03

*For sale by the National Technical Information Service, Springfield, Virginia 22161